DEVELOPMENT OF A HYBRID-ELECTRIC POWER-SYSTEM MODEL FOR A SMALL SURVEILLANCE AIRCRAFT

James R. Harvey*, Robert A. Jarvis*, Dries Verstraete, Richard L. Bagg***, Damon Honnery***, Jennifer L. Palmer***

***Defence Science and Technology Organisation, Australia**
****The University of Sydney**
*****Monash University**

james.harvey@dsto.defence.gov.au; robert.jarvis@dsto.defence.gov.au; dries.verstraete@sydney.edu.au; rlbagg@gmail.com; damon.honnery@monash.edu; jennifer.palmer@dsto.defence.gov.au

Keywords: *unmanned aircraft system, unmanned aerial vehicle, fuel cell, solar cell, model*

Abstract

A power-system model was created in the Matlab/Simulink™ environment to investigate potential performance benefits for tactical unmanned aircraft achievable with hybrid-electric power. Initially, the model was validated against a hardware-in-the-loop simulation including a fuel cell and a battery. The results from the model compared well with the measurements, despite the model's use of simplified input parameters. Photovoltaic cells were then introduced into the model and were found to significantly improve the performance of the power system. For a basic surveillance mission, the solar cells were estimated to provide an energy saving of 59%, despite an increase in aircraft weight.

1 Introduction

Extending the endurance and range of unmanned aerial systems (UAS) is a topic of study worldwide. The desire to enhance mission capabilities, coupled with rising fuel prices and societal demands to reduce the environmental impact of military platforms, has lead to the application of energy-harvesting techniques and the use of other novel energy sources on-board aircraft [1, 2]. Here, a hybrid-electric power system is considered for small tactical UAS.

At a minimum, a hybrid-electric system consists of a high-energy-density generator (*e.g.*, a fuel cell), to support long endurance, and a high-power-density device, such as a battery, to accommodate rapid changes in load and to augment supply during peak demands [3-5]. Such an arrangement reduces cost per unit power and mitigates the stress imposed on the generator by fluctuating loads [5]. Furthermore, the use of a battery permits the capture and storage of energy from the environment (*e.g.*, from photovoltaic (PV) cells, thermoelectric devices and windmilling) to supplement on-board energy stores. This paper describes a method to permit the evaluation of such technologies by use of computer-aided modelling, supported by bench-top characterisation of real devices.

A power-system model (PSM) was developed in the Matlab/Simulink™ environment to evaluate the performance of a hybrid-electric propulsion system suitable for a small tactical UAS. The PSM is a time-averaged quasi-steady-state model and can accommodate various aircraft configurations, power sources, and mission scenarios. A benefit of the PSM is the ability to input simple and readily available data about each component in the power system and still attain a reasonable approximation of the aircraft's actual power usage.

The PSM was tested by simulating a generic UAS mission. Initially, the power system consisted of a fuel cell and battery, and the

PSM's validity was examined by comparing its results with those from a bench-top hardware-in-the-loop (HWIL) simulation. PV cells were then incorporated into the power system, and the additional benefit to the aircraft's performance was investigated.

2 Model overview

The PSM was developed in the Matlab/ Simulink™ environment, and its basic layout is shown in Fig. 1. Currently, it has the capability to model the flow of power through a hybrid-electric system consisting of a fuel cell, battery and PV array. For the results provided here, a simplified aircraft simulation, including a representation of the aircraft's propulsion system, supplied the PSM with the power demand throughout the mission, as well as the location and orientation of the aircraft.

The power-distribution block determines the contribution of the various power sources to the load and can be configured to represent either a series or parallel power-system. In the series arrangement, the fuel cell and PV cells, continuously charge the battery, whilst the battery supplies the entire load. In the parallel arrangement, the fuel cell, PV cells and battery supply the load directly. While the power output of the fuel cell and battery are dependent on the load, the PV cells' power output is dependent on the environmental conditions and the aircraft state and geometry. As a result, the model is structured such that the PV cells supply the maximum power possible and the fuel cell and battery supply the balance of the load.

The PSM does not model transients that would occur in true dynamic systems; thus, the model is quasi-steady state and its output is more representative of relatively long time periods (*i.e.*, minutes rather than seconds).

2.1 Fuel cell

Generic input parameters were used so that any type of fuel cell (polymer-electrolyte membrane, direct methanol, alkaline, *etc.*) can be modelled without requiring modification of the PSM structure. The input parameters for the model are:

- fuel consumption as a function of output power
- rated power
- fuel-tank capacity.

The performance of a fuel cell is dependent on environmental conditions, such as temperature and air pressure, which vary with altitude. To simplify initial PSM tests, it was assumed that the manufacturer provided performance data at an appropriate operating condition and that the on-board conditions did not vary enough throughout the mission to significantly alter the fuel-cell performance.

2.2 Battery

Similar to the fuel-cell model, generic input parameters were used to represent the battery, and

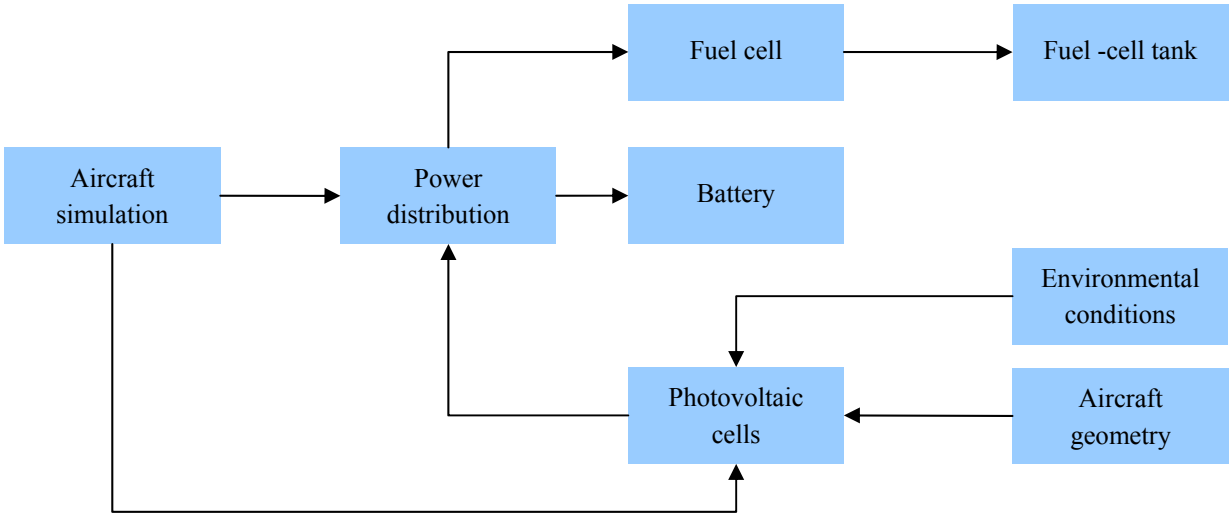

Fig. 1 The flow of information within the PSM structure

it was assumed that the environmental conditions had a negligible effect on its performance.

The input parameters for the battery model are:

- energy capacity as a function of discharge power
- charging power and efficiency
- maximum and minimum allowed states of charge.

2.3 Photovoltaic cells

PV cells require a more sophisticated modelling technique, as their performance is strongly dependent on environmental conditions, as well as on the aircraft state and geometry, as indicated in Fig. 2. The PV model used here is based on the work of Villalva [6, 7] and has been adapted for use on a UAS by Bagg [8].

The fixed input parameters used by the model are:

- maximum power
- current at maximum power point
- voltage at maximum power point
- short-circuit current
- open-circuit voltage
- temperature coefficient at short-circuit current
- temperature coefficient at open-circuit voltage.

Data supplied by PV-cell manufacturers is generally measured at standard conditions (an irradiance of 1000 W/m^2 at the Earth's mid-latitudes and an ambient temperature of 25 °C). Villalva's model constructs a PV-cell characteristic curve at standard conditions [8]. A series of analytical and empirical correlations are then used to adjust the characteristic curve to approximate the PV module's performance at non-standard conditions.

The model's dynamic input parameters are:

- solar irradiance
- cell temperature
- incidence angle.

Solar irradiance and cell temperature are dependent on the environmental conditions in which the aircraft is operating. For the purpose of the tests described herein, the DSTO Environmental-Data Server (DEDS) [9] was used to provide the weather conditions at a particular location and time in history. The values of solar irradiance and ambient temperature output by

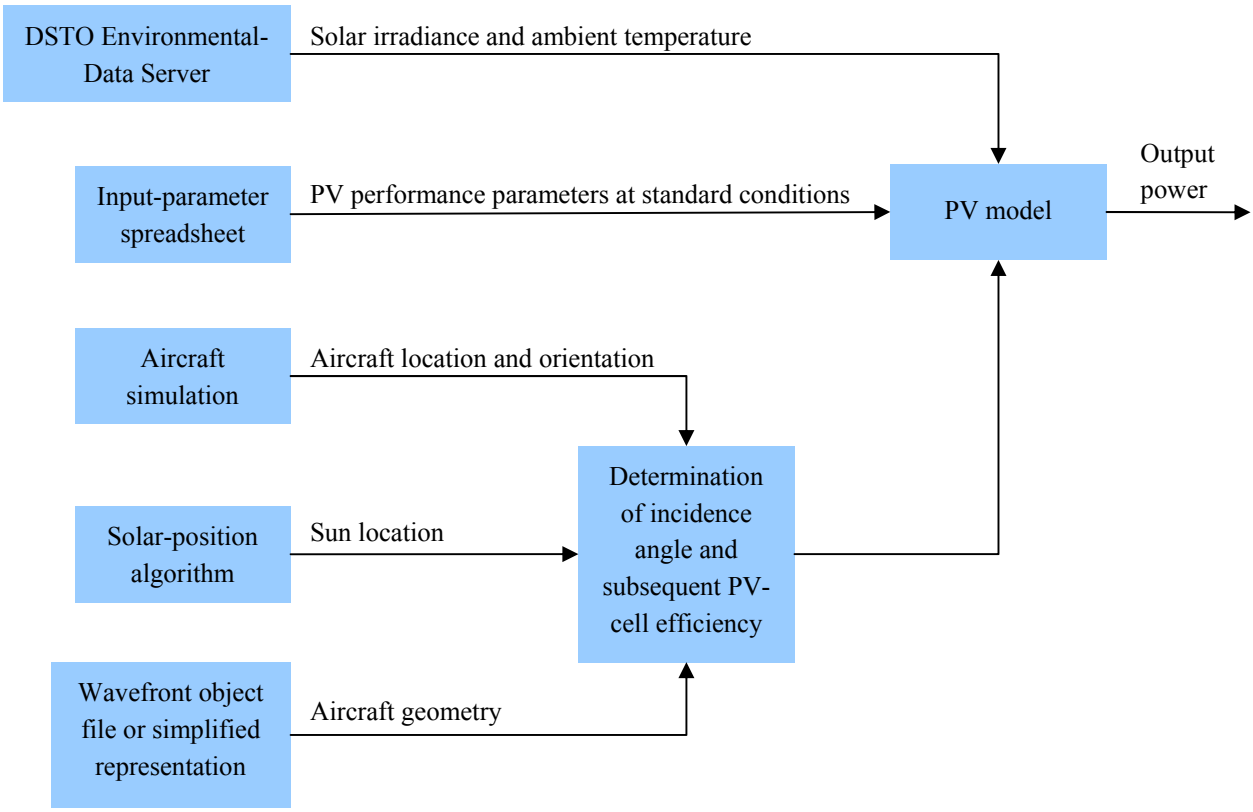

Fig. 2 The structure of the PV model and its various inputs as described in [8]

the DEDS were used by the model at each time step in the simulation, with the PV-cell temperature taken to be the same as the ambient temperature.

Any departure from normal solar incidence reduces the number of incident photons per unit cell, thus reducing cell output power. For an aircraft, the solar-incidence angle is dependent on the orientation of the sun relative to the aircraft, its geometry, and the location of the PV cells on its surface. The location of the sun relative to a fixed frame on the ground was computed using a solar-position algorithm [10], whilst the location and orientation of the aircraft were provided by the simulation. The model only accounted for direct sunlight, and reflections from the ground or other objects were neglected. The reduction in cell efficiency with increasing incidence angle, due to increased reflectivity and apparent junction depth [11], was also neglected.

3 Test I: Validation of PSM against HWIL results

A simplified version of the PSM, including only a fuel cell and battery, was validated by comparing its output with that from a HWIL simulation [12].

3.1 HWIL components

The primary hardware component of the HWIL simulation was an Aeropak fuel-cell system [13], designed specifically for UAS applications and consisting of a polymer-electrolyte-membrane fuel cell and a fuel source. The manufacturer's specifications are given in Table 1.

The Aeropak can be fuelled with compressed hydrogen (H_2) gas or from a hydrogen-gas generator cartridge. The cartridge is filled with a sodium-borohydride ($NaBH_4$) solution that reacts in the presence of a catalyst to produce hydrogen gas and a by-product of sodium borate ($NaBO_2$). The cartridge requires refurbishment after each use; thus, for practicality, a compressed hydrogen cylinder was used in the bench-top experiments [12].

A 6-cell, 1350-mA·h lithium-polymer (LiPo) battery pack is included in the Aeropak system to augment its power output. During a mission, the fuel cell may provide enough power for cruising flight; however, for take-off and climbs, when additional power is required, the battery can increase the power output up to 600 W. The hybrid-electric Aeropak system employs a parallel power-management strategy, where the fuel cell is used as the primary power source and the battery represents the buffer power source. Table 2 summarises the power-management strategy, where P_{FCmax} is the maximum output power of the fuel cell and SOC_{max} and SOC_{min}, are the maximum and minimum states-of-charge of the battery, respectively.

Table 1 Aeropak fuel-cell specifications

Parameter	Value
Fuel-cell stack mass	470 g
No. of cells	35
Rated performance	10 A at 21 V
Continuous output power	200 W
Output voltage range	21–32 V

A programmable electronic load was used to simulate the aircraft's propulsion system. This was a more practical and flexible alternative to using an actual propeller and motor.

3.2 PSM representation

Each component of the HWIL system was represented in the PSM; and, where possible, the input parameters were kept simple. Ideally, the performance of each component would be described only using manufacturer's data, because this would permit the evaluation of the performance of off-the-shelf components in a mission scenario with minimal prior experimentation to obtain input parameters. Unfortunately, this was not always possible, as in some cases insufficient data was provided in the de-

Table 2 Summary of the fuel-cell-based control strategy

Load power	Battery SOC	Action
$> P_{FCmax}$	$< SOC_{min}$	Cannot meet load
$> P_{FCmax}$	$\geq SOC_{min}$	Fuel cell and battery supply load
$< P_{FCmax}$	$< SOC_{max}$	Fuel cell charges battery and supplies load
$< P_{FCmax}$	$\geq SOC_{max}$	Fuel cell supplies load

vice specifications.

It was found through initial experimentation that the Aeropak fuel cell could deliver 270 W, rather than 200 W [12] and that the battery began contributing to the load at 200 W. However, the allocation of power from the fuel cell and battery for loads between 200 W and 270 W has not been documented. As a consequence, the split for loads in this range could not be represented in the PSM. Therefore, for simplicity, it was assumed that the battery only supplied power for a load of 270 W or above.

In addition, the manufacturer provided insufficient data to characterise the Aeropak's fuel consumption; thus, it was measured experimentally [12]. The dependence of fuel consumption on output power was found to be approximately linear, at a rate of 0.01 litres of hydrogen at standard conditions/min/W (sℓ/min/W) or 8.99×10^{-4} g/min/W. Generally, for a fuel cell, the fuel use per unit output power decreases at higher loads; however, this was not observed experimentally for the Aeropak [12].

As previously mentioned, a compressed-hydrogen-gas tank was used in the experiments, rather than a sodium-borohydride cartridge; thus, for the modelling described here, the total mass of hydrogen gas available was taken to be the maximum quantity of hydrogen gas that could be extracted from the standard quantity of sodium-borohydride solution used in a cartridge. This assumption was made to maintain consistency with the Aeropak's use during flight.

The equation for the fuel-cartridge reaction is given by:

$$NaBH_4 + 2H_2O \rightarrow 4H_2 + NaBO_2; \quad (1)$$

and it is known that 250 g of $NaBH_4$ is initially contained in the solution. Therefore, by performing a mass balance, the total amount of hydrogen gas that can be produced was found to be 53.3 g. This is an idealised value, as inefficiencies in the fuel-cartridge system would likely lead to losses of hydrogen gas. The PSM input parameters for the Aeropak fuel cell are summarised in Table 3.

Table 3 PSM input parameters for Aeropak fuel cell

Parameter	Value
Rated power	270 W
Fuel consumption	8.99×10^{-4} g/min/W
H_2-gas-tank capacity	53.3 g

The capacity of a battery generally depends on the current drawn from it. For lead-acid batteries, this dependence is strong; however, for LiPo batteries the dependence is relatively small [14]. Therefore, a simplified constant battery capacity of 1350 mA·h was approximated for use in the PSM.

The Aeropak system includes a constant-current/constant-voltage (CC-CV) battery charger that returns the voltage of each cell to 4 V (rather than 4.2 V – fully charged). To keep the charger simple and light, the manufacturer has not included a cell balancer; therefore, 4 V allowed sufficient latitude to prevent over-charging the cells. Consequently, the battery was observed to recharge to a maximum SOC of approximately 85% in initial testing of the Aeropak. The CC-CV charger operates in two stages. Firstly, the battery is recharged to 4 V/cell at a constant current of 1C (1.35 A) [13]. Then, a constant voltage is maintained and the current is reduced exponentially to a small fraction of the rated current.

Insufficient data was available to model the charging process accurately; therefore, a constant power charge of 32 W was assumed in the PSM, as given by the product of the charging current (1.35 A) and the total nominal voltage of a 6-cell battery with 4 V/cell (24 V). Though not able to accurately represent the charging process, this assumption was believed to reasonably approximate the net power transfer between the fuel cell and battery.

The charge efficiency of LiPo batteries is approximately 90–95% [14]; therefore, a conservative efficiency of 90% was selected for the PSM. Importantly, the battery can be severely damaged if over-discharged; therefore, a conservative SOC lower limit of 40% was selected. The PSM input parameters for the LiPo battery are summarised in Table 4.

As mentioned previously, an electronic load was used to simulate the power sinks, including the propeller and motor, based on a given mission profile.

Table 4 PSM input parameters for LiPo battery

Parameter	Value
Capacity	1350 mA·h
Charge rate	32 W
Charge efficiency	90%
SOC_{max}	85%
SOC_{min}	40%

3.3 Aircraft and mission profile

The target airframe for the power system has the properties shown in Table 5.

A mission typical of this class of aircraft was created for the simulation and used here and by Verstraete *et al.* [12]. As shown in Fig. 3, the mission begins with a warm-up period at 0 W, followed by a maximum-power (600-W) climb and then a 200-W climb to the cruising altitude. Once at the cruising altitude, the UAS loiters at a relatively low power (100 W). During descent, the motor is returned to zero power and during the final approach, flare, and runway taxying, 100 W is assumed to be used for 30 s before the fuel cell is turned off.

3.4 Simulation results

The generic mission shown in Fig. 3 was run in the HWIL simulation [12] and in the PSM. The results obtained in the HWIL simulation [12] and with the PSM are compared in Fig. 4. Fig. 4(a) depicts the fuel-cell output power, while Fig. 4(b) depicts the battery SOC and Fig. 4(c) shows the fuel-cell H_2-gas consumption.

0–180 s

The aircraft is idle for 90 s, and zero power is required from the fuel cell. A small quantity of hydrogen gas is consumed in the HWIL simulation due to purging and the powering of

Table 5 Aircraft properties [15]

Parameter	Value
MTOM	5 kg
Cruise speed	14 m/s
Aspect ratio	13.6
Wing area	0.66 m^2
Wing span	3 m

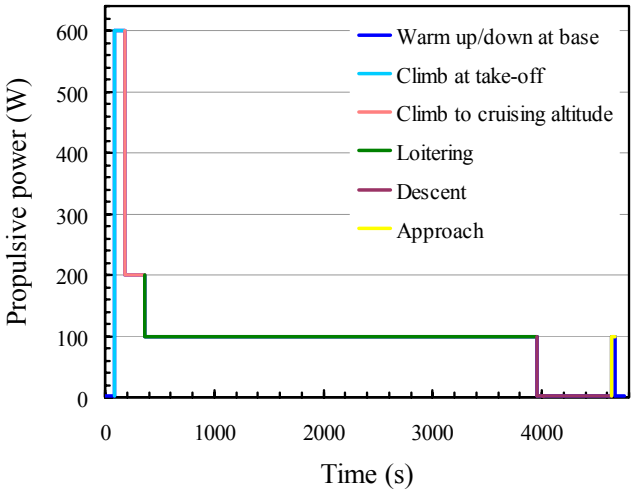

Fig. 3 Generic UAS mission profile

balance-of-plant devices. This is not represented in the PSM results, but the discrepancy is small. At 90 s, take-off commences and the total load increases to 600 W. The maximum rated output power of the fuel cell is produced in the PSM and in the HWIL simulation; and the remaining power is provided by the battery. The steep decline in the battery SOC is captured well by the PSM, as is the fuel consumption.

180–360 s

The aircraft continues to climb, but at a reduced power of 200 W. Currently, the fuel cell has sufficient power to supply the load and to recharge the battery. The fuel-cell power and fuel consumption are reasonably well represented, as is the increase in SOC of the battery.

360–3960 s:

The aircraft cruises at 100 W. Initially, the battery SOC is less than 85%; thus, charging via the fuel cell continues. At approximately 650 s, the battery SOC reaches 85%, charging ceases, and the fuel-cell output power reduces to approximately 100 W. It is evident in Fig. 4(a) and (b) that the PSM does not reproduce the relatively smooth transition from the charging state to the non-charging state. This is due to the assumption of a constant-power charge, which as discussed previously, is not strictly correct. The PSM does, however, provide a reasonable approximation of the net transfer of power between the fuel cell and the battery.

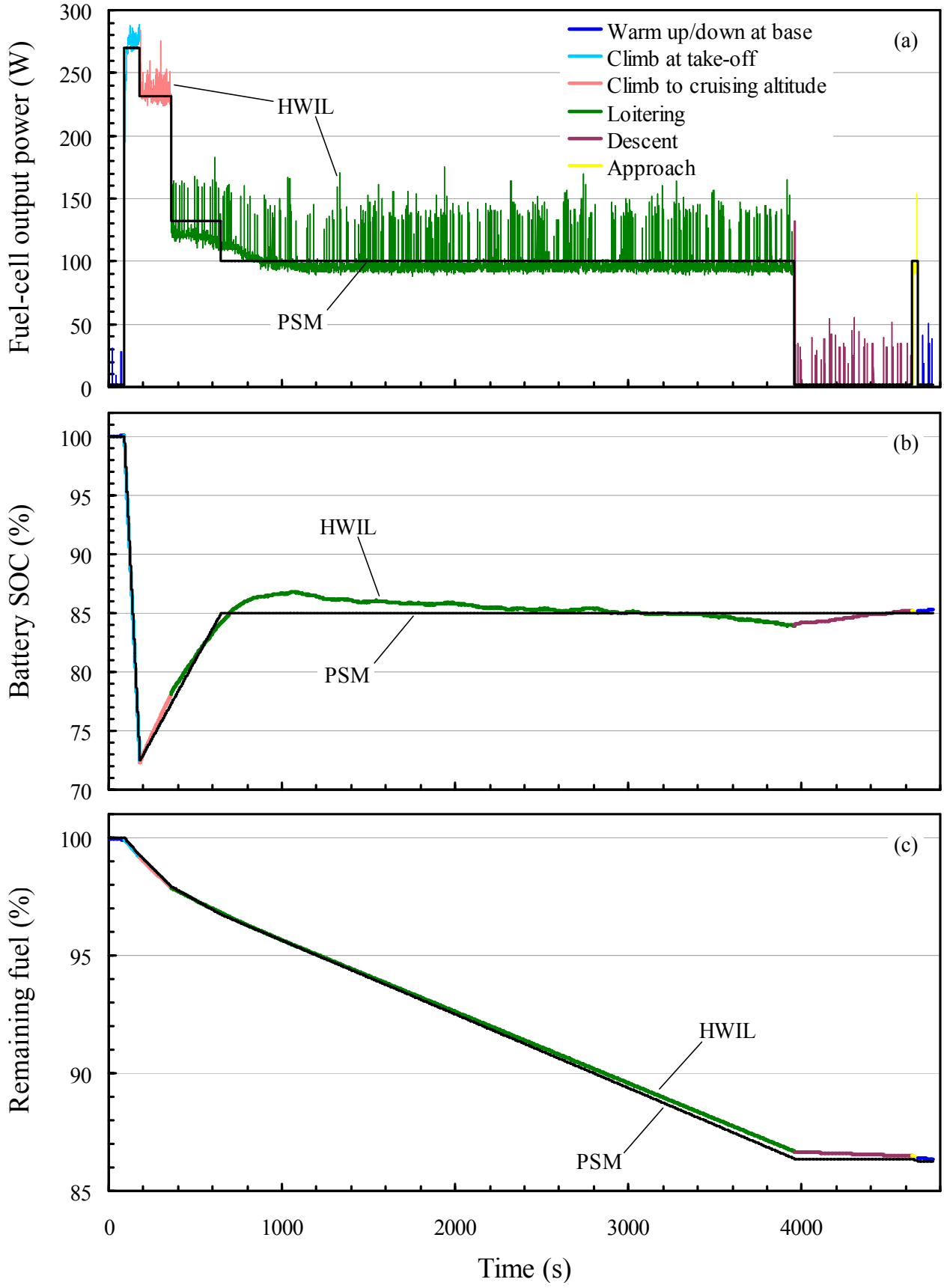

Fig. 4 Comparison of HWIL-simulation and PSM results for (a) fuel-cell-output power, (b) battery SOC, and (c) hydrogen-fuel consumption

3960–5000 s

The period of the aircraft descent and final approach is modelled reasonably well by the PSM.

3.5 Summary of Test I

Overall, the PSM provided a reasonable representation of the HWIL system, despite the use of relatively simple input parameters. Further validation is planned in the future, however, by testing the PSM with a variety of devices and mission profiles.

4 Test II: Investigation of benefits of PV technology

The mission described above was also simulated with PV cells included in the power system. Their benefits to the performance of the aircraft were investigated, accounting for the additional propulsive power required in flight due to the weight of the cells.

4.1 Photovoltaic cells

Sliver® cells, developed by researchers at the Australian National University, are flexible and relatively light and thus suited for integration into an aircraft skin [16, 17]. They were chosen for study as a candidate technology for a future hybrid-electric UAS, and the properties for a 580-cm^2 module (four parallel strings of 125 cells) are listed in Table 6.

For this simulation, the placement of the Sliver® cells was limited to the top and bottom surfaces of the aircraft wings (a total area of 1.32 m^2). It was assumed that the entire wing was covered with a uniform cell density, and that all the cells were identical. To simplify initial PSM tests, the wing was assumed to be a flat plate, where the orientation of each side of the wing was described by a single surface-normal vector, where the normal vector on the top of the wing was equal and opposite to that on the bottom of the wing. A small over-prediction in performance is expected due to this assumption.

Table 6 Properties of Sliver® cells at standard conditions [16, 17]

Parameter	Value
Maximum power	7.04 W
Current at maximum power	0.117 A
Voltage at maximum power	60.0 V
Short circuit current	0.135 A
Open circuit voltage	78.1 V
Current temperature coefficient	1.04×10^{-4} A/ºC
Voltage temperature coefficient	–0.239 V/ºC
Cell density	0.08 kg/m^2

The maximum power point of PV cells is dependent on the radiance incident on them, and thus the orientation of the cells to the sun, and cell temperature. For simplicity, it was assumed that, through the inclusion of maximum power-point trackers of negligible weight, all cells operated at their maximum power points [8]. Further, the effect of clouds and shadows on PV-cell performance was ignored.

4.2 Aircraft simulation

In Sect. 3, only the power demand was used to describe the mission. The PV model, however, requires information about the aircraft's location and orientation throughout the flight to determine the various environmental conditions, including cell temperature, solar irradiance, and the incidence angle on each PV cell. A simple flight path, shown in Fig. 5, was derived to correspond with the power profile given in Fig. 3. Roll, pitch and climb angles typical of the class of aircraft described in Table 5 were chosen for the simulation.

As a consequence of the added weight of the solar cells, a 2% increase in the required propulsive power was approximated using

$$P_2 = P_1 (1 + \Delta m/M_1), \qquad (2)$$

which was based on the derivation by Inman *et al.* in [18]. P_1 and P_2 represent the required propulsive power before and after mass Δm is added, respectively; and M_1 is the initial mass of the aircraft. Though derived for steady-flight conditions, Eq. (2) provided a reasonable approximation. The additional propulsive power required was added to the power profile shown in Fig. 3. The affect of the PV cells on skin-friction drag was neglected.

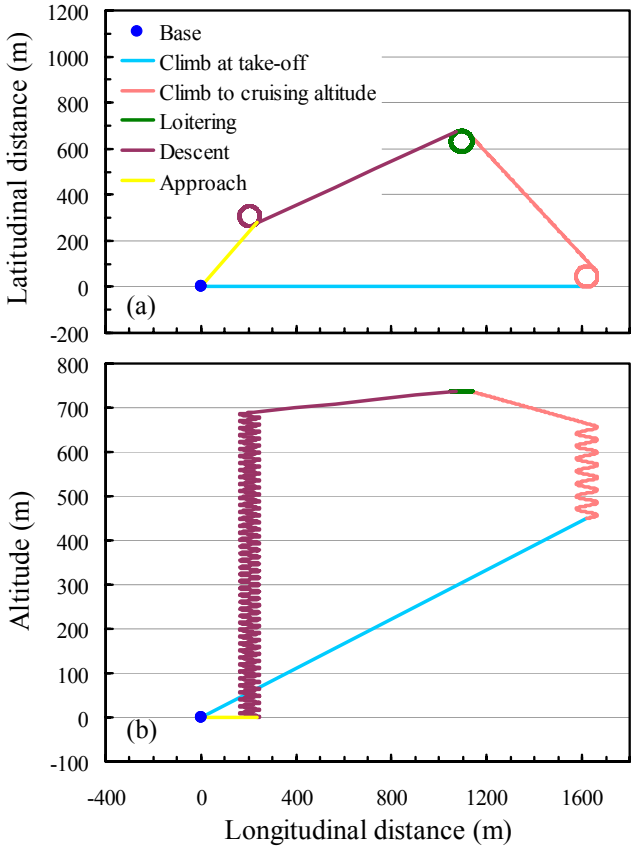

Fig. 5 Aircraft simulation: (a) ground track and (b) altitude variation

4.3 DSTO Environmental-Data Server

For this investigation, the environmental conditions were obtained from a hindcast made by use of the DSTO Environmental-Data Server (DEDS) [9]. The ambient temperature and solar irradiance for 27 March 2010 at 11:00 am local standard time in the Kaipara region of New Zealand were input to the model [19]. The solar irradiance was relatively constant throughout the flight, at 1370 W/m^2; while the ambient temperature varied between 19 ˚C at ground level and 12 ˚C at the maximum altitude of ~740 m, as shown in Fig. 5(b). As previously mentioned, the ambient temperature was assumed to be equal to the PV-cell temperature.

4.4 Simulation results

Fig. 6(a) depicts the PV-cell output power over the course of the mission. The mean power output was 64 W, but was highly variable due to the varying incidence angle, having a standard deviation of 13.4 W. The PV cells on the bottom

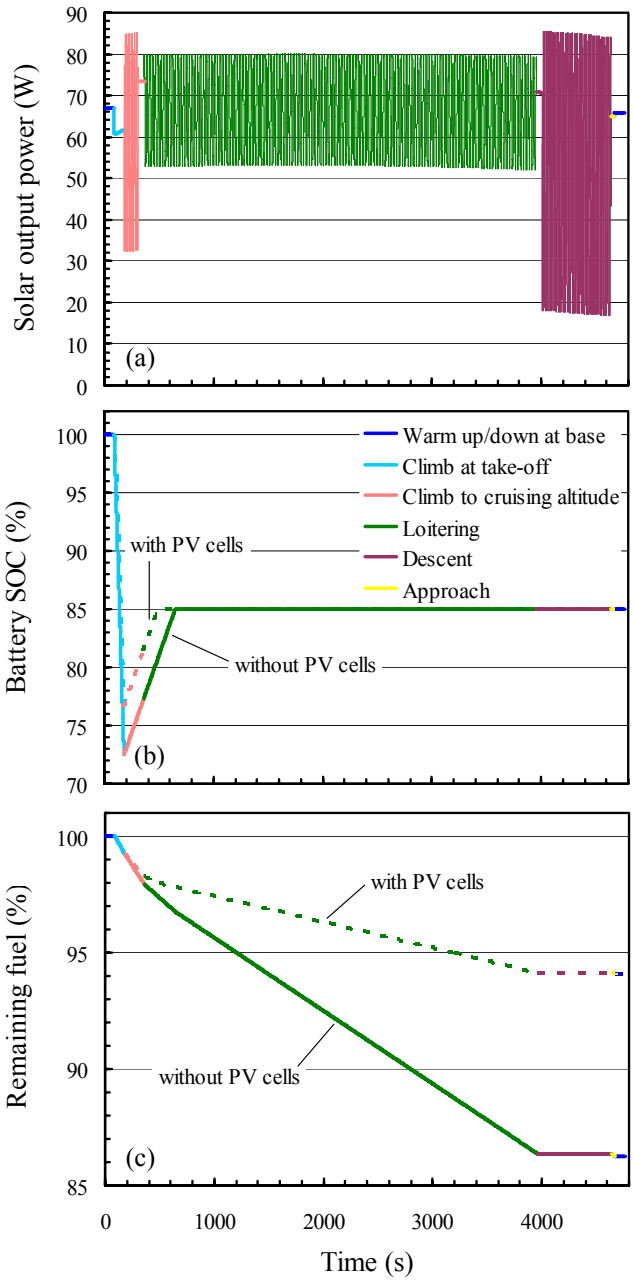

Fig. 6 (a) Total power output of PV cells, along with (b) battery SOC and (c) fuel usage with and without PV cells

surface of the wings did not receive direct solar irradiance at any stage; thus the total power output from the bottom of the wings was 0 W.

The mass of the aircraft could be reduced by removing the PV cells on the bottom of the wings; however, the use of downward pointing PV cells could be advantageous around sunrise and sunset, and might have advantages if the effects of reflected light are taken into consideration. Further investigation is required, however, to determine the feasibility of this configuration for a mission.

Figures 6(b) and (c) compare the PSM-modelled Aeropak fuel consumption and the battery SOC, respectively, with and without the PV cells. Despite the increase in aircraft weight resulting from the addition of the PV cells, a 59% reduction in H_2-fuel use was achieved at the end of the mission, thus demonstrating a significant improvement in the aircraft's maximum endurance.

5 Conclusion

The results of preliminary tests performed using a model of a hybrid-electric power system for a small UAS were presented herein. Initially, the model was validated against a HWIL simulation consisting of a fuel cell and a battery. The results from the model compared well with the measurements, despite the use of relatively simple input parameters being used by the model. The charging of the battery could not be accurately modelled; however, the PSM provided a reasonable approximation of the net transfer of power between the fuel cell and battery.

After initial validation of the model, PV cells were incorporated and were found to significantly improve the performance of the power system for a typical small surveillance aircraft. For the particular aircraft simulation described herein, a H_2-fuel saving of 59% was achieved despite the small increase in weight resulting from the application of PV cells on the aircraft.

References

[1] Palmer JL. Energy alternatives for unmanned aerial vehicles. *Land Warfare Conference 2008*, Brisbane, 2008.

[2] Thomas JP, Qidwai MA, *et al.* Energy scavenging for small-scale unmanned systems. *Journal of Power Sources*, Vol. 159, No. 2, pp. 1494-1509, 2006.

[3] Bernard J, Hofer M, *et al.* Fuel cell/battery passive hybrid power source for electric powertrains. *Journal of Power Sources*, Vol. 196, No. 14, pp. 5867-5872, 2011.

[4] Jeong K-S, Lee W-Y, *et al.* Energy management strategies of a fuel cell/battery hybrid system using fuzzy logics. *Journal of Power Sources*, Vol. 145, No. 2, pp. 319-326, 2005.

[5] Yu Z, Zinger D, *et al.* An innovative optimal power allocation strategy for fuel cell, battery and supercapacitor hybrid electric vehicle. *Journal of Power Sources*, Vol. 196, No. 4, pp. 2351-2359, 2011.

[6] Villalva MG, Gazoli JR, *et al.* Comprehensive approach to modelling and simulation of photovoltaic arrays. *IEEE Transactions on Power Electronics*, Vol. 24, No. 5, 2009.

[7] Villalva MG, Gazoli JR, *et al.* Modelling and circuit-based simulation of photovoltaic arrays. *Brazillian Journal of Power Electronics*, Vol. 14, No. 1, pp. 35-45, 2009.

[8] Bagg RL. *Alternative energy for small unmanned aircraft systems*. B.E. (Aero) thesis, Department of Mechanical Engineering, Monash University, 2011.

[9] Palmer JL, Wharington JM, *et al. The DEDS: DSTO's Environmental-Data Server for research applications*, Defence Science and Technology Organisation, 2012.

[10] Reda I and Andreas A. *Solar position algorithm for solar radiation applications*, National Renewable Energy Laboratory:Colarado, 2008.

[11] Mialhe P, Mouhamed S, *et al.* The solar cell output power dependence on the angle of incident radiation. *Renewable Energy*, Vol. 1, No. 3-4, pp. 519-521, 1991.

[12] Verstraete D, Harvey JR, *et al.* Hardware-in-the-loop simulation of fuel-cell-based hybrid-electrical UAV propulsion. *28th International Congress of the Aeronautical Sciences*, Brisbane, 2012.

[13] Horizon Energy Systems. *The dawn of hydrogen fuel-cell flight*. 2010. Available at: http://www.hes.sg/.

[14] Sauer DU. Batteries: charge-discharge curves. *Encyclopedia of Electrochemical Power Sources*. Elsevier, 2009.

[15] Dawson M. *Fuel-cell-powered aircraft sizing and design*, Defence Science and Technology Organisation, 2012.

[16] Verlinden PJ, Blakers AW, *et al.* Sliver® solar cells: A new thin-crystalline silicon photovoltaic technology. *Solar Energy Materials and Solar Cells*, Vol. 90, No. 18-19, pp. 3422-3430, 2006.

[17] Kerr MJ, Stocks MJ, *et al.* Latest production developments in Sliver technology. *European Photovoltaic Solar Energy Conference* Germany, 2006.

[18] Inman SR and Inman DJ. Performance modelling of unmanned aerial vehicles with on-board energy

harvesting. *Active and Passive Smart Structures and Integrated Systems V*, San Diego, California, USA 2011.

[19] Palmer JL, Ashman DM, *et al.* Preliminary flight testing of autonomous soaring with the Kahu UAS. *AIAC14*, Melbourne, Australia, 2012.

Acknowledgements

The authors wish to express their thanks to Mr. Jon Dansie and Mr. Geoff Brian of the Defence Science and Technology Organisation for their help with the aircraft simulation. Mr. Matthew Dawson of the University of Adelaide is acknowledged for his work on scaling the Kahu aircraft to a suitable size for the simulations contained herein, and Mr. Phil Strong of the New Zealand Defence Technology Agency is acknowledged for his provision of detailed information on the Kahu aircraft system. Dr. Igor Skryabin of the Australian National University Centre for Sustainable Energy Systems is acknowledged for his provision of data on Sliver® cells.

Copyright Statement